ACS OMEGA

http://pubs.acs.org/journal/acsodf

Article

Simultaneous Rapid Nucleic Acid and Protein Detection in a Lateral Chromatography Chip for COVID-19 Diagnosis

Qiuyuan Lin,[‖] Jin Zhang,[‖] Liling Liu, Jilie Kong,* and Xueen Fang*

Cite This: *ACS Omega* 2022, 7, 38409−38416

Read Online

ACCESS | Metrics & More | Article Recommendations | Supporting Information

ABSTRACT: In this work, we report a fast, portable, and economical microfluidic platform for the simultaneous detection of nucleic acid and proteins. Using SARS-CoV-2 as a target, this microfluidic chip enabled to simultaneously detect the SARS-CoV-2 RNA (N gene) antigen (or specific IgG antibody) with respective detection limits of 1 copy/μL for nucleic acid, 0.85 ng/mL for antigen, and 5.80 ng/mL for IgG within 30 min with high stability and anti-interference ability. The capability of this system in clinical applications was further evaluated using clinical samples, displaying 100% sensitivity and 100% specificity for COVID-19 diagnosis. These findings demonstrate the potential of this method to be used for the detection and subsequent control of pathogens.

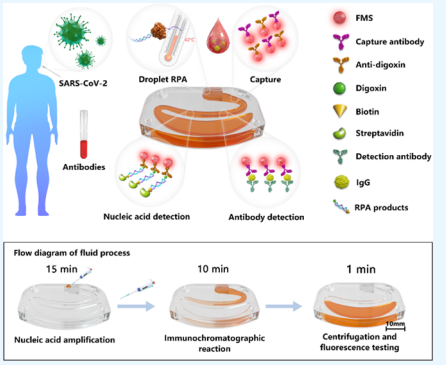

INTRODUCTION

The ability to detect a variety of biomarkers including nucleic acids and proteins plays an important role in clinical diagnostics, drug discovery, environmental monitoring, and food analysis.[1−3] Most current testing methods are limited to detect either a single biomarker or only one type of biomarkers in a single assay.[4] With the development of detection technology, an integrated platform that enables the simultaneous analysis of nucleic acid and protein biomarkers has become extremely attractive and important for satisfying complex testing requirements, which would greatly improve the sensitivity and specificity of the detection technique as well as promote the accuracy of practical applications.[5,6] For example, research data have shown that some patients infected with SARS-CoV-2 are negative for viral RNA;[7−10] meanwhile, the variation of IgM and IgG could be detected as biomarkers after symptom onset. Therefore, it is of great significance to combine the detection of nucleic acid and protein biomarkers not only for COVID-19 but also for other practical diagnostics, which will improve the reliability and accuracy of clinical diagnosis.[11]

So far, there are two main categories of methods for COVID-19 diagnostic: PCR[7,8,12,13] or isothermal nucleic acid amplification-based methods[14−19] detect SARS-CoV-2 viral RNA and serology-based immunoassays detect the SARS-CoV-2-specific antigen or antibodies (such as IgG and IgM).[10,20−24] In addition, various nucleic acid amplification-assisted point-of-care diagnostics have been recently developed for targeting SARS-CoV-2 RNA, including minimally instrumented SHERLOCK testing,[25] smartphone fluorescence readout system,[26] and lateral flow strips.[27−29] Among them, recombinase polymerase amplification (RPA) is an alternative isothermal amplification (37 °C) method instead of PCR with the outstanding advantages of rapidness and high sensitivity. The RPA assay coupled with microfluidic lateral chromatography was recently developed for the detection of SARS-CoV-2 RNA with a high sensitivity of 1 copy/μL and a run time of 30 min. This method, however, was unable to detect RNA and antibodies simultaneously.[14] Our group has recently developed an immunomicrofluidic chip for the detection of the SARS-CoV-2 antigen, IgM, and IgG, but it fails to combine the detection of SARS-CoV-2 RNA.[20] Many platforms for simultaneous rapid nucleic acid and protein detection such as a gold nanoparticle probe-based microarray,[30] a dye-encoded bead-based array,[5] and a lateral flow nucleic acid biosensor[31] were built for simultaneous visual detection of nucleic acids and proteins but only allowed for detection of the relatively high concentration of nucleic acids (~pM) due to the inability to amplification of nucleic acid targets, thereby limiting their further application. Recently, a label-free nanoplasmonic biosensor was reported for detecting nucleic acid, spike protein, and antibodies together for COVID-19 screening;[32] however, it relies on a long time for nucleic acid hybridization without amplification ability, resulting in limited efficiency and sensitivity for clinical applications. It is thus still

Received: June 4, 2022
Accepted: August 16, 2022
Published: October 21, 2022

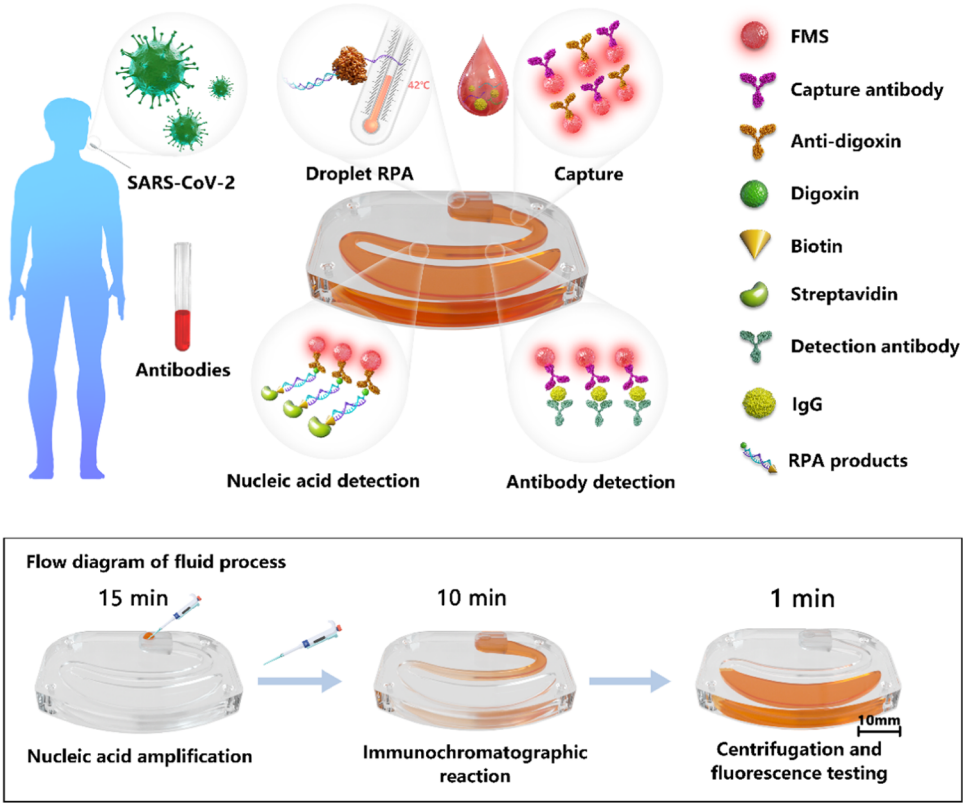

Figure 1. Schematic of the microfluidic chip platform for the simultaneous detection of nucleic acid and proteins using SARS-CoV-2 as a proof-of-concept target. (The images in the figure are free domain).

demanded to develop an integrated platform for the rapid, simple, sensitive, cost-effective, and simultaneous detection of nucleic acid and protein biomarkers, achieving precise diagnoses in response to complex clinical situations.

Here, we report a portable point-of-care lateral chromatography chip platform that enables the simultaneous detection of nucleic acid and proteins in a single-reaction chip. Details of the microfluidic chip design, construction, preparation, and assembly are described in the Supporting Information. Briefly, this fabricated chip comprises a sample loading chamber for sample loading and RPA nucleic acid amplification, an "S-shaped" channel for the lateral chromatographic reaction, including a capture zone and two test zones, and a waste reservoir for waste collection (Figures 1 and S1). The RPA reaction was able to effectively amplify the nucleic acid target, thereby improving the detection sensitivity. This developed lateral chromatography chip assay for simultaneous nucleic acid and protein detection was demonstrated using SARS-CoV-2 RNA, SARS-CoV-2 antigen, or IgG as targets. Capture antibodies for the SARS-CoV-2 antigen or IgG and anti-digoxin antibodies for RPA amplicons were labeled with fluorescent microspheres (FMSs) separately and functioned as the detection signal. A mixture of these FMS-labeled antibodies was patterned on the capture zone of the microfluidic chip for the specific capture of corresponding targets. Detection antibodies for the SARS-CoV-2 antigen or IgG and streptavidin for RPA amplicons were patterned in the test zones of the microfluidic chip (details are given in the Supporting Information).

RESULTS AND DISCUSSION

Principle of Simultaneous Nucleic Acid and Protein Detection on the Lateral Chromatography Chip. The basic principle of this lateral chromatography microfluidic system is illustrated in Figure 1. Using SARS-CoV-2 as a target, the microfluidic chip assay was composed of nucleic acid amplification, immunochromatographic reaction for simultaneous nucleic acid and protein detection on the microfluidic chip, and centrifugation and fluorescence signal readout by a portable device (Figure S1B). Briefly, this assay included the following steps: (1) add nuclei acid sample and seal with a waterproof membrane; (2) incubate for 15 min at 42 °C in a heating incubator; (3) tear off the waterproof membrane and add the protein sample (in the case of IgG or antigen); (4) seal with the waterproof membrane again and allow the chromatography reaction for 10 min; and (5) insert a cassette into a portable analyzer for centrifugation and automatic readout.

First, the RPA reaction for amplifying nucleic acid was carried out in a sealed sample loading chamber at 42 °C for 15 min with a droplet of the nucleic acid sample (from the pharyngeal swab sample) mixed with the RPA reaction solution to 5 μL. The sequences of the RPA primers and the SARS-CoV-2 N gene used in this study are listed in Table S1. The forward primer and the reverse primer were synthesized and modified with digoxin and biotin, respectively, at five terminals for the lateral chromatography reaction in microfluidic chips. After the RPA reaction, 20 μL of the clinical protein sample (i.e., serum sample for IgGs or pharyngeal swab sample for the antigen) mixed with 80 μL of sample buffer was then added to the sample loading chamber, and the chamber

https://doi.org/10.1021/acsomega.2c03499
ACS Omega 2022, 7, 38409−38416

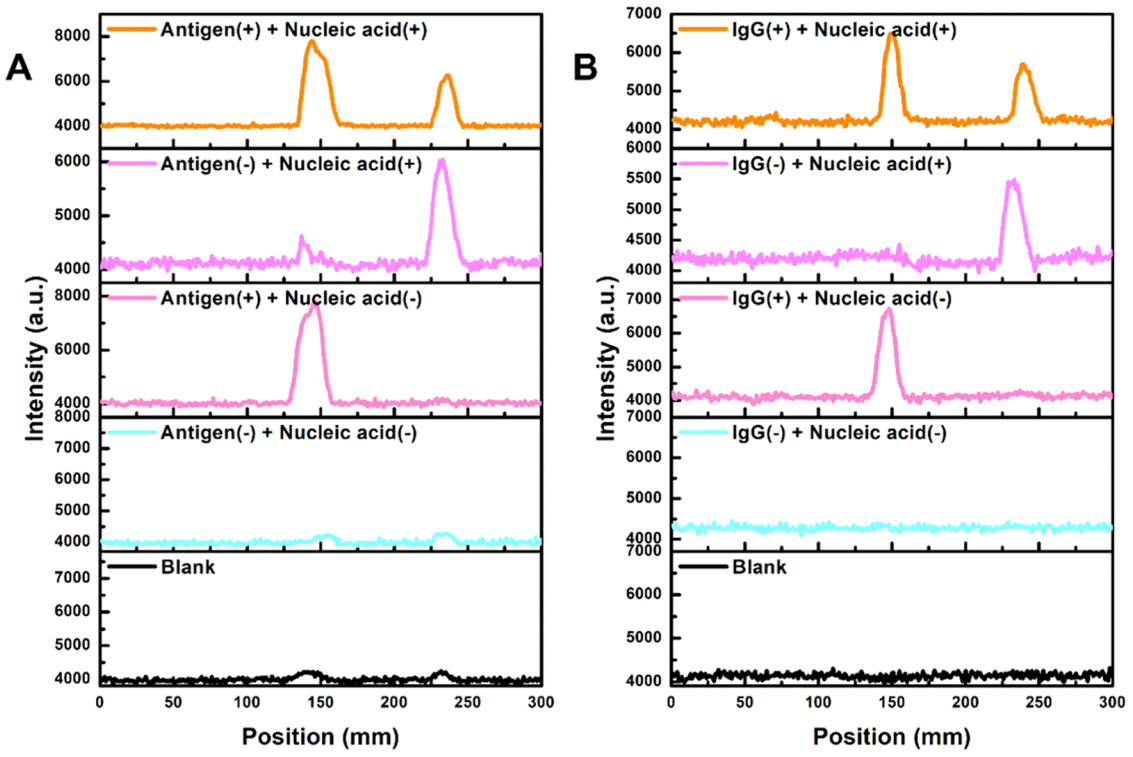

Figure 2. Fluorescence signal curves for the simultaneous detection of nucleic acid and proteins on a microfluidic chip (A) using the SARS-CoV-2 N gene and antigen as a target (B) using the SARS-CoV-2 N gene and IgG. Nucleic acid (−) indicates an RPA reaction without the SARS-CoV-2 N gene, Nucleic acid (+) indicates an RPA reaction with the SARS-CoV-2 N gene (1000 copies/μL), Antigen (−) indicates 0 ng/mL of antigen, Antigen (+) indicates 150 ng/mL of antigen, IgG (−) indicates 0 ng/mL of IgG, and IgG (+) indicates 1000 ng/mL of IgG. The RPA reaction was performed at 42 °C for 15 min in the microfluidic chip. The lateral chromatography reaction was then performed at room temperature for 10 min. Blank (negative control) indicates that only sample buffer was added. The first test zone (~150 mm) is for the antigen or IgG, and the second test zone (~230 mm) is for RPA amplicons. Each experiment was repeated three times.

was quickly sealed with a waterproof and breathable membrane to prevent aerosol contamination while ensuring liquid flow. As the liquid flowed over the capture zone, the SARS-CoV-2 protein biomarker (antigen or antibody) and RPA amplicons with digoxin-modified terminals were specifically recognized and captured by the corresponding FMS-labeled capture antibodies. Less FMS-labeled capture antibodies than detection antibodies were absorbed on the surface of the microfluidic chip, which was because there was a smaller interaction area ratio between FMS-labeled capture antibodies and the surface of the microfluidic chip than that between detection antibodies and the surface of the microfluidic chip due to the large nanoparticle size of FMSs (200 nm). Therefore, except for partial adsorption on the capture zone due to electrostatic adsorption and hydrophobic force, most FMS-labeled antibodies that have weak or no interaction with the microfluidic chip are easily detached from the microchip and migrated with the flow under capillary action. When the liquid flows over the first protein test zone, FMSs captured with targets become immobilized by detection antibodies through antigen−antibody interactions. It is worth mentioning that enough detection antibodies remain attached to the surface of the microfluidic chip for detection because of the larger interaction area ratio between detection antibodies and the surface of the microfluidic chip than that between FMS-labeled capture antibodies and the surface of the microfluidic chip. Subsequently, the biotin-modified terminal of RPA amplicons was bound by streptavidin and formed a sandwich-type immunocomplex in the second nucleic acid test zone. After 10 min, for the lateral chromatography assay at room temperature, the microfluidic chips were placed in the portable fluorescence analyzer followed by a centrifugation step (2000 rpm, 10 s) to remove residual liquids and minimize nonspecific adsorption. Finally, the original fluorescence signal is recorded with the wavelengths of excitation and emission at 360 and 610 nm, respectively. Three microfluidic chips can be simultaneously tested along with data processing, analysis, and result output on the portable instrument in a single operation in 1 min. The entire process from sample application to the result takes less than 30 min, eliminating multiple washing steps, greatly simplifying the operation, and reducing time and cost.

Feasibility of Simultaneous Detection of Nucleic Acid and Proteins on the Lateral Chromatography Chip. The lateral chromatography chip for the simultaneous detection of nucleic acid and proteins was first validated by standard samples using the combination of the SARS-CoV-2 N gene and antigen or IgG as a target. For simultaneous detection of the SARS-CoV-2 N gene and antigen, as shown in Figure 2A, applying 100 μL of sample buffer without RPA amplicons and protein (blank) did not generate a signal in either the first protein test zone (at ~150 mm) or the second nucleic acid test zone (at ~230 mm, black curve). Antigen-positive and -negative samples in combination with an RPA reaction of 1000 copies/μL N gene template (nucleic acid positive) were tested in the microfluidic chip. In the first test zone, a strong fluorescence signal was detected for the antigen-positive sample (orange curve) and no signal was detected for the

https://doi.org/10.1021/acsomega.2c03499
ACS Omega 2022, 7, 38409−38416

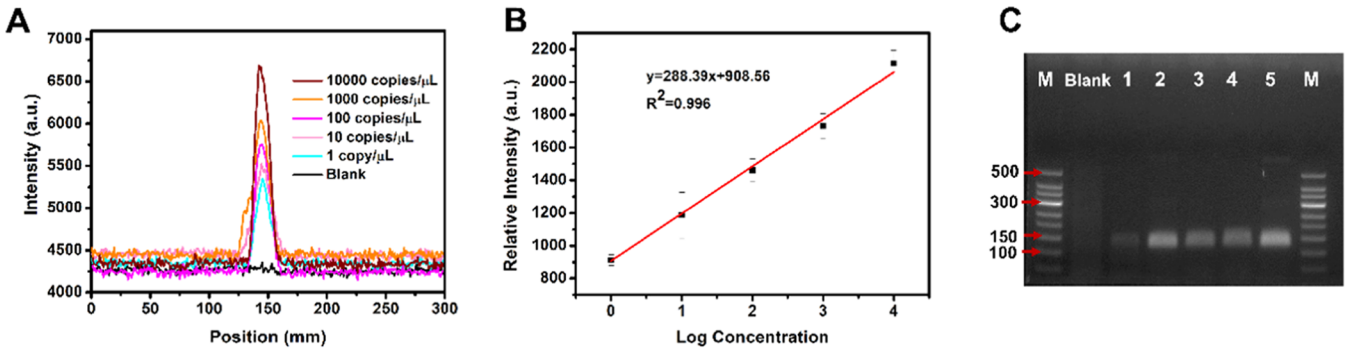

Figure 3. (A) Fluorescence signal generated by serial dilutions of the SARS-CoV-2 N gene (1−10 000 copies/μL) based on the RPA-lateral chromatography assay using a microfluidic chip. Each RPA reaction (5 μL total volume) was carried out on a microfluidic chip at 42 °C for 15 min. Each concentration was tested three times. The lateral chromatography reaction was performed at room temperature for 10 min. (B) The linearity between relative intensity and the logarithmic value of the target concentration. (C) Electrophoresis pattern of RPA amplicons of the standard samples. The fragment length of the RPA products was 120 bp. M: DNA marker, blank: negative control (ultrapure water), and 1−5: the initial concentration of the target from 1 to 10 000 copies/μL.

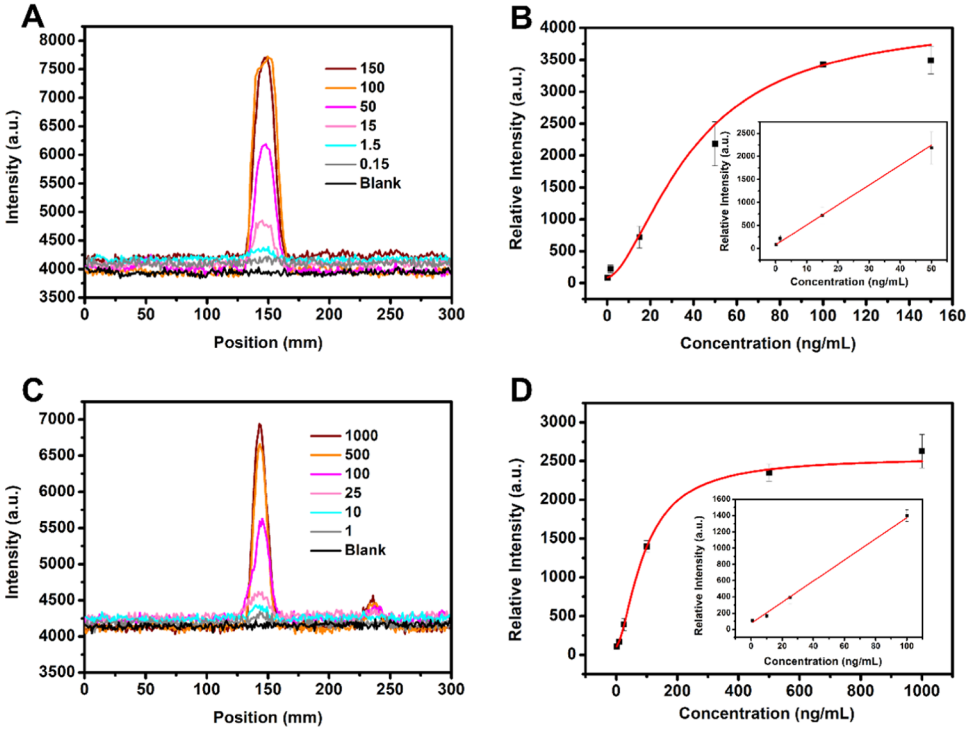

Figure 4. (A) Evaluation of the performance of the microfluidic chip method using the serial dilution standard antigen samples (0.15, 1.5, 15, 50, 100, and 150 ng/mL). (B) Corresponding calibration curve between the antigen concentration and relative intensity. The inset figure shows the linear relationship between the antigen concentration and the fluorescence intensity ranging from 0.15 to 50 ng/mL. (C) Evaluation of the performance of the microfluidic chip method using the serial dilution standard IgG samples (1, 10, 25, 100, 500, and 1000 ng/mL). (D) Corresponding calibration curve between the IgG concentration and fluorescence intensity. The inset figure shows the linear relationship between the IgG concentration and the fluorescence intensity ranging from 1 to 100 ng/mL. The lateral chromatography reaction was performed at room temperature for 10 min. Blank: negative control (PBS). Each concentration was tested three times.

antigen-negative sample (magenta curve). A significant RPA signal was generated in the second test zone (orange and magenta curves). Similarly, when antigen-positive and -negative samples in combination with the RPA reaction without the SARS-CoV-2 N gene (nucleic acid negative) were detected in the microfluidic chip, a strong fluorescence signal was obtained for the antigen-positive sample (pink curve) and no signal was observed for the antigen-negative sample (blue curve) in the first test zone. The second test zone did not produce a significant signal (pink and blue curves) because the samples were nucleic acid-negative. Similar results were obtained for simultaneous detection of the SARS-CoV-2 N gene and IgG (Figure 2B), indicating that this integrated approach is capable of simultaneously detecting nucleic acid and proteins, potentially enhancing the accuracy and sensitivity of diagnosis.

RPA Assay for Nucleic Acid Detection. Next, the detection sensitivity of a single RPA reaction was explored for SARS-CoV-2 detection using the chip system. The SARS-CoV-2 N gene was serially diluted to final concentrations of 1, 10, 100, 1000, and 10 000 copies/μL in the RPA reaction buffer. A 5 μL aliquot of each standard sample was reacted at

https://doi.org/10.1021/acsomega.2c03499
ACS Omega 2022, 7, 38409−38416

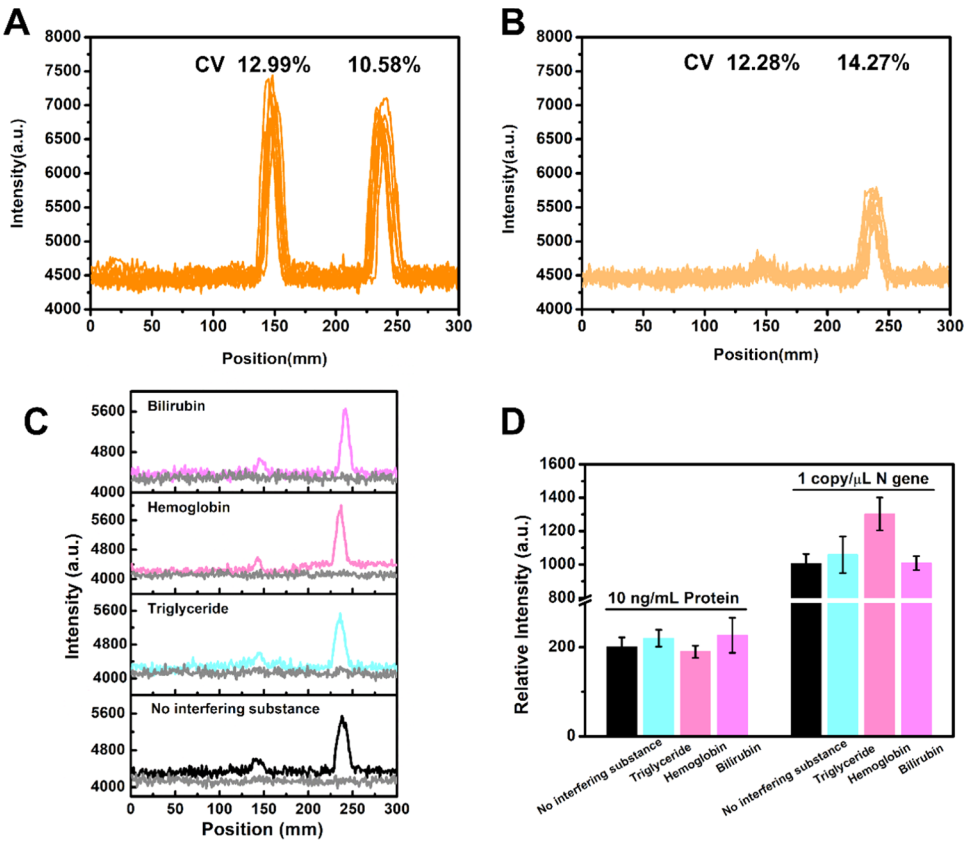

Figure 5. Reproducibility was evaluated by 10 replicate experiments using (A) high-concentration samples (IgG 1000 ng/mL, SARS-CoV-2 N gene 10 000 copies/μL) and (B) low-concentration samples (IgG 1 ng/mL, SARS-CoV-2 N gene 1 copy/μL). (C) Interference assessment of the microfluidic chip in the presence of 3 mg/mL triglycerides, 0.5 mg/mL hemoglobin, and 0.05 mg/mL bilirubin. Positive samples (curves with two signal peaks): the final concentrations of IgG and SARS-CoV-2 N gene were 10 ng/mL and 1 copy/μL, respectively; negative control (gray curve): blank without IgG and SARS-CoV-2 N gene targets. The RPA reaction was performed at 42 °C for 15 min in the microfluidic chip; the lateral chromatography reaction was then performed at room temperature for 10 min. The first test zone was for IgG (~150 mm), and the second test zone was for RPA amplicon (~230 mm). (D) The relative intensity of positive samples tested by microfluidic chips in the presence or absence of 3 mg/mL triglycerides, 0.5 mg/mL hemoglobin, and 0.05 mg/mL bilirubin. Each experiment was repeated three times.

42 °C for 15 min. Next, 100 μL of the sample buffer was added to each of the chips to allow the RPA amplicons to flow through the test zone; the immunoassay was allowed to react for 10 min. The first test zone was designed for detecting nucleic acid. The detection results are shown in Figure 3A. The target at all dilutions from 1 to 10 000 copies/μL generated an increasing fluorescence signal in the first test zone (~150 mm), while no signal was detected in the second test zone (~230 mm). These results demonstrate that our microfluidic chip platform is capable of detecting nucleic acid with single-copy sensitivity. The results in Figure 3B demonstrate a good linear relationship between the relative intensity and the logarithmic value of the target concentration (range 1−10 000 copies/μL, R^2 = 0.996). The relative intensity was automatically calculated from the strongest peak intensity minus the background intensity, which was obtained directly from the instrument (see details in the Supporting Information). The electrophoresis results of the RPA amplicons (120 bp) generated at 42 °C for 15 min in PCR tubes (Figure 3C) further demonstrate the feasibility and single-copy sensitivity of the microfluidic chip-based immuno-RPA method.

Protein (Antigen or IgG) Assay. We also investigated the performance of the microfluidic chip method for detecting protein biomarkers using the SARS-CoV-2-specific antigen and IgG as targets. The standard SARS-CoV-2 antigen was diluted in PBS to 0.15, 1.5, 15, 50, 100, and 150 ng/mL and was tested using microfluidic chips (10 min, room temperature). Figure 4A shows the fluorescence curves of the different concentrations of the antigen. There was no or very low signal in the second test zone for nucleic acid detection. A significant relationship between the antigen concentration and fluorescence intensity was observed—$y = 4142.72 - 4053.35/(1 + (x/39.921)^{1.657})$, R^2 = 0.998; 0.15−150 ng/mL: $y = 81.03 + 43.25x$, R^2 = 0.951 (Figure 4B). The limit of detection (LOD) was 0.85 ng/mL, which was calculated as LOD = mean of the blank + 3σ (where σ is the standard deviation). Similarly, the detection sensitivity for IgG was assessed by our immunomicrofluidic chip (Figure 4C,D). The fitting curves show a good relationship between the IgG concentration and relative intensity: 1−1000 ng/mL: $y = 2553.22 - 2448.37/(1 + (x/93.172)^{1.579})$, R^2 = 0.998; 1−100 ng/mL: $y = 75.15 + 12.99x$, R^2 = 0.986 (Figure 4D). The limit of detection (LOD) was 5.80 ng/mL. These results demonstrated the quantitative detection capability of this platform over a wide concentration range.

Detection Performance of the Lateral Chromatography Chip. Stability is important for a diagnostic method. The fluorescence intensity of capture antibody-modified FMSs showed a strong fluorescence signal as pure FMSs under the same concentration (Figure S2A). The stability of this platform

https://doi.org/10.1021/acsomega.2c03499
ACS Omega 2022, 7, 38409−38416

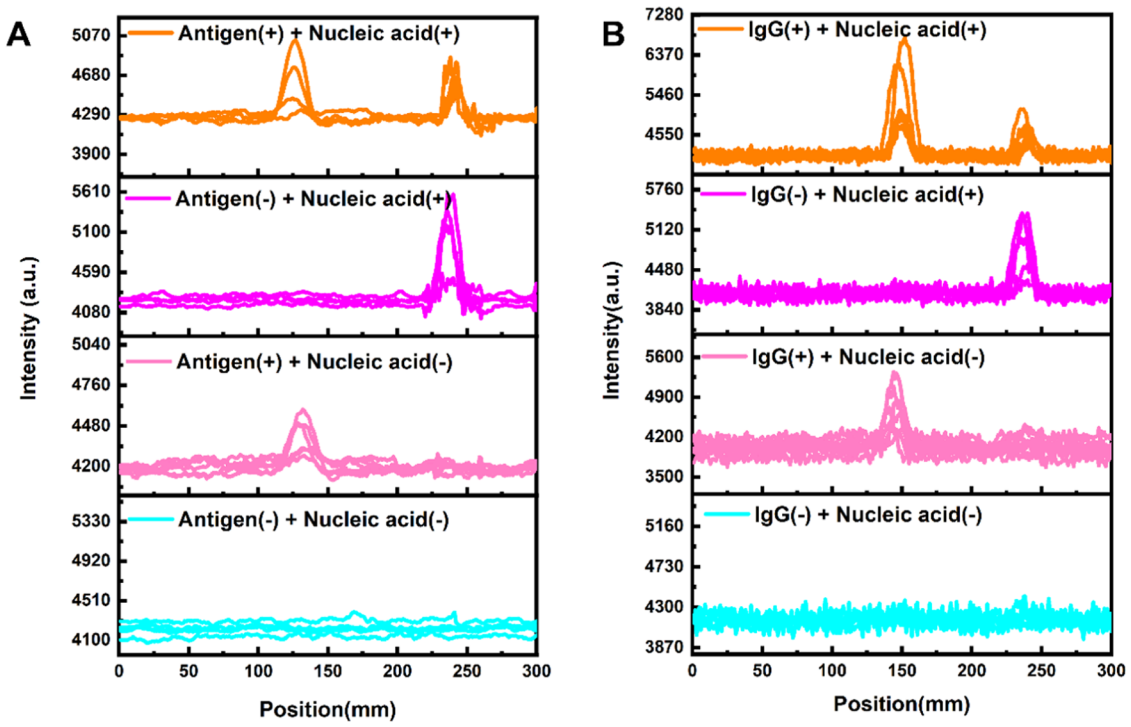

Figure 6. Evaluating applicability of the microfluidic chip for clinical samples. (A) Fluorescence signal curves for the simultaneous detection of the antigen and SARS-CoV-2 RNA. (B) Fluorescence signal curves for the simultaneous detection of IgG and SARS-CoV-2 RNA. Antigen (−) + Nucleic acid (−), Antigen (+) + Nucleic acid (−), Antigen (−) + Nucleic acid (+), and Antigen (+) + Nucleic acid (+), respectively, indicates five, six, four, and four groups of nasopharyngeal swab samples and RNA samples from COVID-19-negative or -positive patients. IgG (−) + Nucleic acid (−), IgG (+) + Nucleic acid (−), IgG (−) + Nucleic acid (+), and IgG (+) + Nucleic acid (+), respectively, indicate five, seven, five, and seven groups of serum samples and RNA samples from COVID-19-negative or -positive patients. Antigen (−) + Nucleic acid (−): five groups of nasopharyngeal swab samples and RNA samples from COVID-19-negative patients. (−) and (+) indicate negative and positive samples, respectively. The RPA reaction was performed at 42 °C for 15 min in the microfluidic chip, and then 20 μL of the nasopharyngeal swab sample or serum sample was mixed with 80 μL of the sample buffer and added to the chip. The lateral chromatography reaction was allowed to proceed at room temperature for 10 min. The first test zone was for the antigen (∼130 mm) or IgG (∼150 mm), and the second test zone was for RPA amplicons (∼230 mm).

was also tested on the 0, 1st, 3rd, and 7th days using the prepared microfluidic chips from the same batch. As shown in Figure S2B, the tested concentration from 0 to 7 days was close to theoretical concentration, indicating that the fluorescence signal, as well as the prepared microfluidic chips, has good stability. Furthermore, the developed assay was evaluated by simultaneously detecting high- (1000 ng/mL protein and 10 000 copies/μL SARS-CoV-2 N gene) and low-concentration samples (1 ng/mL protein and 1 copy/μL SARS-CoV-2 N gene). Figure 5A,B shows the results of 10 replicate experiments using high- and low-concentration samples. The relative intensity of these replicate experiments is obtained in Figure S3A,B, respectively. The interassay coefficients of variation (CVs) for the high-concentration samples were 12.99 and 10.58%, and the CVs of low-concentration samples were 12.28 and 14.27%, indicating the relatively good stability and repeatability of this approach.

The lack of interference is also an important performance parameter, as many interfering substances typically found in clinical samples can affect the accuracy of detection. As common interfering substances, triglycerides, hemoglobin, and bilirubin at the maximum clinical dose were used to evaluate the level of interference in the microfluidic chip when simultaneously detecting nucleic acid (1 copy/μL SARS-CoV-2 N gene) and protein (10 ng/mL IgG). Figure 5C,D shows that the interference of these substances is negligible toward simultaneous detection of the SARS-CoV-2 N gene and IgG, indicating that the method has good selectivity and is robust to interference.

Simultaneous Detection of SARS-CoV-2 RNA and Protein in Clinical Samples. In this study, the combined detection of the protein and nucleic acid by our platform was evaluated by clinical samples, including nasopharyngeal swab samples (n = 19) for antigen detection, serum samples (n = 24) for IgG detection, and RNA samples extracted from nasopharyngeal swab samples (n = 24) for SARS-CoV-2 RNA detection. All clinical samples were provided and tested by the Qingdao Administration of Entry & Exit Inspection and Quarantine Bureau (Qingdao, China). Figure 6A displays the simultaneous detection of the antigen and SARS-CoV-2 RNA. No signal was observed for the antigen or SARS-CoV-2 RNA from COVID-19-negative individuals (n = 5). When six positive antigen samples and six negative RNA samples were tested, a fluorescence signal for the antigen was generated in the first test zone, while there was no signal in the second zone. Similarly, four negative antigen samples and four positive RNA samples generated only the SARS-CoV-2 RNA signal in the second test zone. Furthermore, the fluorescence signal from both antigen and SARS-CoV-2 RNA was detected for four positive antigen samples and four positive RNA samples. Results were also obtained for detecting IgG and SARS-CoV-2. As shown in Figure 6B, no signal was observed for IgG or

https://doi.org/10.1021/acsomega.2c03499
ACS Omega 2022, 7, 38409−38416

SARS-CoV-2 RNA from COVID-19-negative individuals (n = 5). Seven positive serum samples and seven negative RNA samples were tested. A fluorescence signal for IgG was generated in the first test zone, while there was no signal in the second zone. Similarly, five negative serum samples and five positive RNA samples generated only the SARS-CoV-2 RNA signal in the second test zone. Furthermore, a fluorescence signal from both IgG and SARS-CoV-2 RNA was detected for seven positive serum samples and seven positive RNA samples. The results of the two sets of detection (a total of 43 cases) are listed in Table S2 and Figure S4. The receiver operating characteristic (ROC) curves are further obtained in Figure S5. Cutoff values for antigen, IgG, and RNA detection were identified as 51.27 ± 2.56 (95% confidence interval), 262.0 ± 13.10, and 137.7 ± 6.89, respectively (relative intensity) according to ROC curves. Based on the cutoff values, detection results by this developed method (Table S2 and Figure S4) were consistent with clinical diagnosis, demonstrating 100% sensitivity and 100% specificity for diagnosing COVID-19 (Table 1), which were calculated according to the following standard: a positive COVID-19 diagnosis was made when at least either RNA or IgG (antigen) test was determined as positive. These results indicate the high consistency of our assay with clinically confirmed results, suggesting that this chip-based lateral chromatography assay has strong potential for the simultaneous detection of the antigen or IgG (a protein biomarker) and SARS-CoV-2 RNA for COVID-19 diagnosis.

Table 1. Comparison of the Developed Microfluidic Method and Clinical Diagnosis Results[a]

		this method		
		positive	negative	total
clinical diagnosis	positive	33	0	33
	negative	0	10	10
total		33	10	43

[a]Sensitivity = 33/(33 + 0) × 100% = 100% and specificity = 10/(0 + 10) × 100% = 100%.

CONCLUSIONS

In summary, we developed a lateral chromatography chip for the simultaneous detection of nucleic acid and proteins. An RPA assay and an immunoassay were realized using a single chip. The developed chip was evaluated and used to diagnose COVID-19. The results obtained with this method were highly consistent with clinical diagnosis results. This easy-to-use method enables multibiomarker detection with high sensitivity and rapidity (30 min). This low-cost, point-of-care pathogen screening method has potential applications in a range of medical diagnostics.

ASSOCIATED CONTENT

Supporting Information

The Supporting Information is available free of charge at https://pubs.acs.org/doi/10.1021/acsomega.2c03499.

Experimental section; supporting tables (Table S1 and S2); and supporting figures (Figures S1−S5) (PDF)

AUTHOR INFORMATION

Corresponding Authors

Jilie Kong − *Department of Chemistry and Institutes of Biomedical Sciences, Fudan University, Shanghai 200433, P. R. China*; Email: jlkong@fudan.edu.cn

Xueen Fang − *Department of Chemistry and Institutes of Biomedical Sciences, Fudan University, Shanghai 200433, P. R. China*; orcid.org/0000-0002-3266-7868; Email: fxech@fudan.edu.cn

Authors

Qiuyuan Lin − *Department of Chemistry and Institutes of Biomedical Sciences, Fudan University, Shanghai 200433, P. R. China*

Jin Zhang − *Qingdao International Travel Healthcare Center, Qingdao Customs, Qingdao 266071, P. R. China*

Liling Liu − *Shanghai Suxin Biotechnology Co. Ltd., and IgeneTec Diagnostic Products Co. Ltd., Shanghai 201318, P. R. China*

Complete contact information is available at: https://pubs.acs.org/10.1021/acsomega.2c03499

Author Contributions

‖Q.L. and J.Z. contributed equally to this work. All authors have given approval to the final version of the manuscript.

Notes

The authors declare no competing financial interest.

ACKNOWLEDGMENTS

We gratefully acknowledge the financial support by the Shanghai Agricultural Development project (2021-02-08-00-12-F00772 to X.F.) and National Natural Science Foundation of China (21974028 and 22174024 to X.F.; 22174022 and 22127806 to J.K.).

REFERENCES

(1) Lin, M.; Song, P.; Zhou, G.; Zuo, X.; Aldalbahi, A.; Lou, X.; Shi, J.; Fan, C. Electrochemical detection of nucleic acids, proteins, small molecules and cells using a DNA-nanostructure-based universal biosensing platform. *Nat. Protoc.* **2016**, *11*, 1244−1263.

(2) Cohen, L.; Walt, D. R. Single-Molecule Arrays for Protein and Nucleic Acid Analysis. *Annu. Rev. Anal. Chem.* **2017**, *10*, 345−363.

(3) Li, Y.-F.; Sun, Y.-M.; Beier, R. C.; Lei, H.-T.; Gee, S.; Hammock, B. D.; Wang, H.; Wang, Z.; Sun, X.; Shen, Y.-D.; Yang, J.-Y.; Xu, Z.-L. Immunochemical techniques for multianalyte analysis of chemical residues in food and the environment: A review. *TrAC, Trends Anal. Chem.* **2017**, *88*, 25−40.

(4) Huang, Y.; Cheng, Z.; Han, R.; Gao, X.; Qian, L.; Wen, Y.; Zhang, X.; Liu, G. Target-induced molecular-switch on triple-helix DNA-functionalized carbon nanotubes for simultaneous visual detection of nucleic acids and proteins. *Chem. Commun.* **2020**, *56*, 13657−13660.

(5) Wang, X.; Walt, D. R. Simultaneous detection of small molecules, proteins and microRNAs using single molecule arrays. *Chem. Sci.* **2020**, *11*, 7896−7903.

(6) Mao, X.; Gurung, A.; Xu, H.; Baloda, M.; He, Y.; Liu, G. Simultaneous detection of nucleic acid and protein using gold nanoparticles and lateral flow device. *Anal. Sci.* **2014**, *30*, 637−642.

(7) Ravi, N.; Cortade, D. L.; Ng, E.; Wang, S. X. Diagnostics for SARS-CoV-2 detection: A comprehensive review of the FDA-EUA COVID-19 testing landscape. *Biosens. Bioelectron.* **2020**, *165*, No. 112454.

(8) Feng, W.; Newbigging, A. M.; Le, C.; Pang, B.; Peng, H.; Cao, Y.; Wu, J.; Abbas, G.; Song, J.; Wang, D.-B.; Cui, M.; Tao, J.; Tyrrell, D. L.; Zhang, X.-E.; Zhang, H.; Le, X. C. Molecular Diagnosis of

COVID-19: Challenges and Research Needs. *Anal. Chem.* **2020**, *92*, 10196−10209.
(9) Wiersinga, W. J.; Rhodes, A.; Cheng, A. C.; Peacock, S. J.; Prescott, H. C. Pathophysiology, Transmission, Diagnosis, and Treatment of Coronavirus Disease 2019 (COVID-19): A Review. *JAMA* **2020**, *324*, 782−793.
(10) Norman, M.; Gilboa, T.; Ogata, A. F.; Maley, A. M.; Cohen, L.; Busch, E. L.; Lazarovits, R.; Mao, C.-P.; Cai, Y.; Zhang, J.; Feldman, J. E.; Hauser, B. M.; Caradonna, T. M.; Chen, B.; Schmidt, A. G.; Alter, G.; Charles, R. C.; Ryan, E. T.; Walt, D. R. Ultrasensitive high-resolution profiling of early seroconversion in patients with COVID-19. *Nat. Biomed. Eng.* **2020**, *4*, 1180−1187.
(11) Carter, L. J.; Garner, L. V.; Smoot, J. W.; Li, Y.; Zhou, Q.; Saveson, C. J.; Sasso, J. M.; Gregg, A. C.; Soares, D. J.; Beskid, T. R.; Jervey, S. R.; Liu, C. Assay Techniques and Test Development for COVID-19 Diagnosis. *ACS Cent. Sci.* **2020**, *6*, 591−605.
(12) Corman, V. M.; Landt, O.; Kaiser, M.; Molenkamp, R.; Meijer, A.; Chu, D. K. W.; Bleicker, T.; Brünink, S.; Schneider, J.; Schmidt, M. L.; Mulders, D. G. J. C.; Haagmans, B. L.; Veer, B. V. D.; Brink, S. V. D.; Wijsman, L.; Goderski, G.; Romette, J. L.; Ellis, J.; Zambon, M.; Peiris, M.; et al. Detection of 2019 novel coronavirus (2019-nCoV) by real-time RT-PCR. *Eurosurveillance* **2020**, *25*, No. 2000045.
(13) Pfefferle, S.; Reucher, S.; Nörz, D. S.; Lütgehetmann, M. Evaluation of a quantitative RT-PCR assay for the detection of the emerging coronavirus SARS-CoV-2 using a high throughput system. *Eurosurveillance* **2020**, *25*, No. 2000152.
(14) Liu, D.; Shen, H.; Zhang, Y.; Shen, D.; Zhu, M.; Song, Y.; Zhu, Z.; Yang, C. A microfluidic-integrated lateral flow recombinase polymerase amplification (MI-IF-RPA) assay for rapid COVID-19 detection. *Lab Chip* **2021**, *21*, 2019−2026.
(15) Xun, G.; Lane, S. T.; Petrov, V. A.; Pepa, B. E.; Zhao, H. A rapid, accurate, scalable, and portable testing system for COVID-19 diagnosis. *Nat. Commun.* **2021**, *12*, No. 2905.
(16) Yu, L.; Wu, S.; Hao, X.; Dong, X.; Mao, L.; Pelechano, V.; Chen, W.-H.; Yin, X. Rapid Detection of COVID-19 Coronavirus Using a Reverse Transcriptional Loop-Mediated Isothermal Amplification (RT-LAMP) Diagnostic Platform. *Clin. Chem.* **2020**, *66*, 975−977.
(17) Thi, V. L. D.; Herbst, K.; Boerner, K.; Meurer, M.; Kremer, L. P. M.; Kirrmaier, D.; Freistaedter, A.; Papagiannidis, D.; Galmozzi, C.; Stanifer, M. L.; Boulant, S.; Klein, S.; Chlanda, P.; Khalid, D.; Miranda, I. B.; Schnitzler, P.; Kräusslich, H. G.; Knop, M.; Anders, S. A colorimetric RT-LAMP assay and LAMP-sequencing for detecting SARS-CoV-2 RNA in clinical samples. *Sci. Transl. Med.* **2020**, *12*, No. eabc7075.
(18) Qian, J.; Boswell, S. A.; Chidley, C.; Lu, Z.-X.; Pettit, M. E.; Gaudio, B. L.; Fajnzylber, J. M.; Ingram, R. T.; Ward, R. H.; Li, J. Z.; Springer, M. An enhanced isothermal amplification assay for viral detection. *Nat. Commun.* **2020**, *11*, No. 5920.
(19) Xia, S.; Chen, X. Single-copy sensitive, field-deployable, and simultaneous dual-gene detection of SARS-CoV-2 RNA via modified RT−RPA. *Cell Discovery* **2020**, *6*, 37.
(20) Lin, Q.; Wen, D.; Wu, J.; Liu, L.; Wu, W.; Fang, X.; Kong, J. Microfluidic Immunoassays for Sensitive and Simultaneous Detection of IgG/IgM/Antigen of SARS-CoV-2 within 15 min. *Anal. Chem.* **2020**, *92*, 9454−9458.
(21) Van Elslande, J.; Houben, E.; Depypere, M.; Brackenier, A.; Desmet, S.; André, E.; Van Ranst, M.; Lagrou, K.; Vermeersch, P. Diagnostic performance of seven rapid IgG/IgM antibody tests and the Euroimmun IgA/IgG ELISA in COVID-19 patients. *Clin. Microbiol. Infect.* **2020**, *26*, 1082−1087.
(22) Li, Z.; Yi, Y.; Luo, X.; Xiong, N.; Liu, Y.; Li, S.; Sun, R.; Wang, Y.; Hu, B.; Chen, W.; Zhang, Y.; Wang, J.; Huang, B.; Lin, Y.; Yang, J.; Cai, W.; Wang, X.; Cheng, J.; Chen, Z.; Sun, K.; et al. Development and clinical application of a rapid IgM-IgG combined antibody test for SARS-CoV-2 infection diagnosis. *J. Med. Virol.* **2020**, *92*, 1518−1524.
(23) Chen, Z.; Zhang, Z.; Zhai, X.; Li, Y.; Lin, L.; Zhao, H.; Bian, L.; Li, P.; Yu, L.; Wu, Y.; Lin, G. Rapid and Sensitive Detection of anti-SARS-CoV-2 IgG, Using Lanthanide-Doped Nanoparticles-Based Lateral Flow Immunoassay. *Anal. Chem.* **2020**, *92*, 7226−7231.
(24) Amanat, F.; Stadlbauer, D.; Strohmeier, S.; Nguyen, T. H. O.; Chromikova, V.; McMahon, M.; Jiang, K.; Arunkumar, G. A.; Jurczyszak, D.; Polanco, J.; Bermudez-Gonzalez, M.; Kleiner, G.; Aydillo, T.; Miorin, L.; Fierer, D. S.; Lugo, L. A.; Kojic, E. M.; Stoever, J.; Liu, S. T. H.; Cunningham-Rundles, C.; et al. A serological assay to detect SARS-CoV-2 seroconversion in humans. *Nat. Med.* **2020**, *26*, 1033−1036.
(25) de Puig, H.; Lee Rose, A.; Najjar, D.; Tan, X.; Soenksen Luis, R.; Angenent-Mari Nicolaas, M.; Donghia Nina, M.; Weckman Nicole, E.; Ory, A.; Ng Carlos, F.; Nguyen Peter, Q.; Mao Angelo, S.; Ferrante Thomas, C.; Lansberry, G.; Sallum, H.; Niemi, J.; Collins James, J. Minimally instrumented SHERLOCK (miSHERLOCK) for CRISPR-based point-of-care diagnosis of SARS-CoV-2 and emerging variants. *Sci. Adv.* **2021**, *7*, No. eabh2944.
(26) Ning, B.; Yu, T.; Zhang, S.; Huang, Z.; Tian, D.; Lin, Z.; Niu, A.; Golden, N.; Hensley, K.; Threeton, B.; et al. A smartphone-read ultrasensitive and quantitative saliva test for COVID-19. *Sci. Adv.* **2021**, *7*, No. eabe3703.
(27) Broughton, J. P.; Deng, X.; Yu, G.; Fasching, C. L.; Servellita, V.; Singh, J.; Miao, X.; Streithorst, J. A.; Granados, A.; Sotomayor-Gonzalez, A.; et al. CRISPR−Cas12-based detection of SARS-CoV-2. *Nat. Biotechnol.* **2020**, *38*, 870−874.
(28) Patchsung, M.; Jantarug, K.; Pattama, A.; Aphicho, K.; Suraritdechachai, S.; Meesawat, P.; Sappakhaw, K.; Leelahakorn, N.; Ruenkam, T.; Wongsatit, T.; et al. Clinical validation of a Cas13-based assay for the detection of SARS-CoV-2 RNA. *Nat. Biomed. Eng.* **2020**, *4*, 1140−1149.
(29) Ali, Z.; Sánchez, E.; Tehseen, M.; Mahas, A.; Marsic, T.; Aman, R.; Sivakrishna Rao, G.; Alhamlan, F. S.; Alsanea, M. S.; Al-Qahtani, A. A.; Hamdan, S.; Mahfouz, M. Bio-SCAN: A CRISPR/dCas9-Based Lateral Flow Assay for Rapid, Specific, and Sensitive Detection of SARS-CoV-2. *ACS Synth. Biol.* **2022**, *11*, 406−419.
(30) Scott, A. W.; Garimella, V.; Calabrese, C. M.; Mirkin, C. A. Universal Biotin−PEG-linked gold nanoparticle probes for the simultaneous detection of nucleic acids and proteins. *Bioconjugate Chem.* **2017**, *28*, 203−211.
(31) Huang, Y.; Cheng, Z.; Han, R.; Gao, X.; Qian, L.; Wen, Y.; Zhang, X.; Liu, G. Target-induced molecular-switch on triple-helix DNA-functionalized carbon nanotubes for simultaneous visual detection of nucleic acids and proteins. *Chem. Commun.* **2020**, *56*, 13657−13660.
(32) Masterson, A. N.; Muhoberac, B. B.; Gopinadhan, A.; Wilde, D. J.; Deiss, F. T.; John, C. C.; Sardar, R. Multiplexed and High-Throughput Label-Free Detection of RNA/Spike Protein/IgG/IgM Biomarkers of SARS-CoV-2 Infection Utilizing Nanoplasmonic Biosensors. *Anal. Chem.* **2021**, *93*, 8754−8763.

https://doi.org/10.1021/acsomega.2c03499
ACS Omega 2022, 7, 38409−38416